Oscillations and Traveling Waves of Calcium: A Simplified Model

Benjamin Singer

Department of Mathematics, University of Michigan, 525 East University Avenue, Ann Arbor, MI, 48109-1109, USA.

James Sneyd

I.I.M.S., Massey University Albany Campus, Auckland, N.Z.
j.sneyd@massey.ac.nz

Abstract

We construct a heuristic model of calcium oscillations in pancreatic acinar cells. The model is based on the two-state model of Sneyd *et al.* (Sneyd, J., A. LeBeau and D. Yule, 2000, Traveling waves of calcium in pancreatic acinar cells: model construction and bifurcation analysis, *Physica D*, in press) and is similar in spirit to the FitzHugh reduction of the Hodgkin-Huxley equations. The simplified model successfully reproduces the oscillatory behavior and wave behaviour of the more complex model. In particular, the simplified model provides an example of a simple, physiologically relevant model that has a T-point and an associated spiral branch of homoclinic orbits.

1 Introduction

The mechanisms and patterns of cytosolic calcium (Ca^{2+}) release are of great interest to both experimentalists and theoreticians. Intracellular Ca^{2+} oscillations have been observed in a wide variety of cell types, indicating that Ca^{2+} is an important biochemical signal. Two principal types of Ca^{2+} oscillations have been characterized in a variety of cell types: baseline spikes and sinusoid oscillations. The baseline spike is a repeated series of spikes in cytosolic calcium concentration. Each spike consists of a sudden elevation in cytosolic Ca^{2+} level, followed by a rapid return to the baseline concentration. The sinusoidal oscillation, on the other hand, is a sustained elevation of Ca^{2+} concentration with high frequency, low amplitude oscillations about the elevated baseline. The baseline spike is of particular interest because of its possible use as a biochemical signal (Berridge and Galione, 1988; Rooney and Thomas, 1993). The amplitude of the baseline spike is approximately constant at different agonist concentrations, but its frequency is variable and sensitive even to extremely low agonist concentrations. The highly organized nature of the Ca^{2+} oscillation in time makes the baseline spike an easily detectable signal, even against a background of stochastic variation in cytosolic Ca^{2+} concentration and leakage of calcium from cellular Ca^{2+} stores (Thomas *et al.*, 1996).

Much of the interest in Ca^{2+} oscillations results not only from the temporal organization of the Ca^{2+} signal but also from its spatial organization. Traveling waves of elevated Ca^{2+} concentration have been observed in diverse cell types, including hepatocytes, pancreatic acinar cells, and oocytes, in a variety of species (Brezprozvanny and Ehrlich, 1995; Nathanson *et al.*, 1992; Parys *et al.*, 1992; Petersen *et al.*, 1991; Thomas *et al.*, 1996). Since Ca^{2+} diffuses only a few micrometers through the cytosol, the presence of spatially organized waves indicates that the waves must be regenerative in nature. The regenerative mechanism by which waves propagate involves the autocatalyic release of calcium from the endoplasmic reticulum (ER) or sarcoplasmic reticulum (SR), a process often called Ca^{2+}-induced Ca^{2+} release, or CICR (Clapham, 1995). The two principal pathways of CICR are through the ryanodine receptor or the inositol (1,4,5)-trisphosphate (IP_3) receptor. In the case of the IP_3 receptor, which is found predominantly in nonmuscle cells, the receptor mediates interaction between an agonist, such as a hormone or a neurotransmitter, and intracellular stores of

Ca^{2+} such as the ER. When an extracellular agonist binds to the cellular surface, it can stimulate the production of IP_3. This is accomplished via a G-protein link from the surface receptor to the protein phospholipase C, which cleaves phosphotidylinositol(4,5)-bisphosphate into diacylglycerol and IP_3. The IP_3 which is released then diffuses through the cell cytoplasm and interacts with IP_3 receptors on the ER membrane, causing them to open and release Ca^{2+} from the membrane-enclosed stores.

The behavior of the IP_3 receptor itself is also affected by cytosolic Ca^{2+}, with Ca^{2+} both promoting and inhibiting Ca^{2+} release, but at different rates. The study of the IP_3 receptor and its role in Ca^{2+} release is thus an important step toward understanding calcium dynamics at the cellular level.

LeBeau *et al.* (1999) present a model of the IP_3 receptor based on the behavior of observed Ca^{2+} oscillations in pancreatic acinar cells. The model reproduces differing types of Ca^{2+} oscillations in response to different agonists, and also makes several predictions of receptor behavior, predictions that were successfully tested. A variation on the model is presented by Sneyd *et al.* (2000). Although it exhibits interesting and physiologically realistic behavior, the form of the model equations makes analysis prohibitively difficult. It is thus very desirable to develop a model which exhibits the same behavior, without such complex functional forms. We take a heuristic approach to simplifying the model. In the spirit of the FitzHugh reduction of the Hodgkin-Huxley equations, we reproduce the behavior of the model by using functional forms completely unrelated to the physiology upon which the original model was based. We then demonstrate that the heuristic simplification exhibits the same behavior as the physiologically based model of Ca^{2+} oscillations in pancreatic acinar cells, and is thus a useful simplification.

What is particularly interesting is that our simplification is a simple model of an excitable system that has a form different to that of the usual FitzHugh-Nagumo model of excitability. Such unusual excitable systems have been observed previously in models of calcium oscillations, and thus the model presented here will, we hope, provide a convenient way of studying such systems.

2   Models of calcium oscillations

Several approaches have been taken to modeling IP_3-mediated calcium dynamics. The various approaches differ considerably in the assumptions regarding the physiological mechanism of Ca^{2+} release. One of the earliest physiological schemes assumed the existence of two distinct Ca^{2+} stores in the cell, and is therefore known as the two pool model. In the two pool model, one of the stores ("pools") of calcium is assumed to be sensitive to Ca^{2+}, and the other to IP_3 (Kuba and Takeshita, 1981; Goldbeter *et al.*, 1990; Goldbeter, 1996). Recent work has shown that the model applies equally well to a single pool mediated by both Ca^{2+} and IP_3 (Dupont and Goldbeter, 1993, 1994). While the two pool model is based on assumptions regarding whole-cell physiology, several other approaches utilize a more detailed model of the IP_3 receptor. The model of DeYoung and Keizer (1992) assumes that the IP_3 receptor is composed of three independent subunits, each of which has a binding site for IP_3, an activating binding site for Ca^{2+}, and an inactivating binding site for Ca^{2+}, giving a total of eight possible states for each subunit. A simplified model is constructed by assuming that binding at the IP_3 and activating Ca^{2+} binding sites is fast compared to the binding of calcium to the inactivating Ca^{2+} site (DeYoung and Keizer, 1992; Keizer and DeYoung, 1994; Li and Rinzel, Tang *et al.*, 1996). A third, heuristic approach has also been taken to modeling the IP_3 receptor (Atri *et al.*, 1993). A detailed discussion and comparison of the models of Ca^{2+} release can be found in Keener and Sneyd (1998).

More recent experimental work, particularly on the modulation and kinetics of the IP_3 receptor, have shown all these above models to be incorrect in detail, thus stimulating the construction of further models, one of the most recent being due to LeBeau *et al.* (1999).
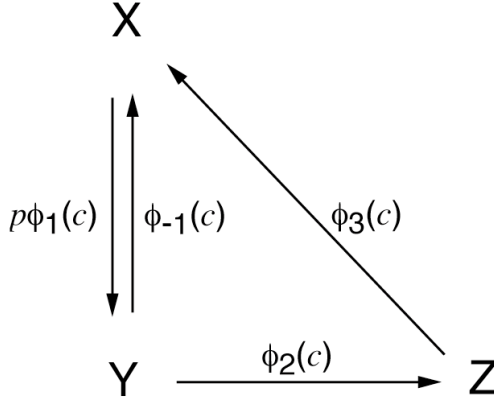
Figure 1: Schematic diagram of the simplified receptor model, showing the possible states of the IP$_3$ receptor, and the transitions between them.

2.1 The two-state receptor model

Modeling the IP$_3$ receptor is further complicated by the sensitivity of the receptor mechanism to the type of agonist used to stimulate Ca^{2+} oscillations. LeBeau *et al.* (1999) present a model which mimics the different types of oscillations induced by acetylcholine (ACh) or cholecystokinin (CCK) in pancreatic acinar cells and make several successfully tested predictions. The model assumes that the IP$_3$ receptor has open, shut, and inactivated states, denoted S, O, and I. A six state model is derived based on the proposal that each state has two variants, with high and low IP$_3$ affinity, and that Ca^{2+} mediates the interconversion of these variants, denoted S and $\tilde{\text{S}}$, and so on for the other states (Hajnóczky and Thomas, 1997; Cardy *et al.*, 1997). By assuming that interconversion between high and low IP$_3$ affinity variants is fast compared to the opening, shutting, or inactivation of the receptor, the authors formulate the *three state model.* By further assuming that opening of the receptor is fast compared to inactivation and recovery from inactivation, the model is further reduced to the *two-state model.* Although Sneyd *et al.* (2000) give a detailed derivation of the model equations, we repeat part of that derivation for the sake of clarity.

The binding diagram of the three-state model is given in Fig. 1; X denotes a shut state of the receptor, Y an open state, and Z an inactivated state. The functions ϕ that control the movement between the receptor states are themselves derived from a more general six-state model, and take the form

$$\phi_1(c) = \frac{k_1 R_1 + r_2 c}{R_1 + c}, \tag{1}$$

$$\phi_{-1}(c) = \frac{(k_{-1} + r_{-2}) R_3}{c + R_3}, \tag{2}$$

$$\phi_2(c) = \frac{k_2 R_3 + r_4 c}{R_3 + c}, \tag{3}$$

$$\phi_3(c) = \frac{k_3 R_5 + r_6 c}{R_5 + c}, \tag{4}$$

where all the ks, Rs and rs are constants. Letting x denote the proportion of receptors in state X, and similarly for y and z, then gives

$$\frac{dx}{dt} = \phi_{-1}(c) y - p \phi_1(c) x + \phi_3(c) z, \tag{5}$$

$$\frac{dy}{dt} \quad = \quad p\phi_1(c)x - \phi_{-1}(c)y - \phi_2(c)y, \tag{6}$$

$$z \quad = \quad 1 - x - y, \tag{7}$$

where p is the concentration of IP_3. Note that IP_3 is involved only in the transition from the shut state to the open state.

It is known that the IP_3 receptor consists of four subunits. If we make the simplifying assumption that these four subunits are identical and independent, then the open probability, P, of the receptor, is given by

$$P = y^4. \tag{8}$$

Finally, we assume that opening of the receptor by IP_3 binding is a fast process compared to receptor inactivation and recovery from inactivation. This is a standard assumption used in many models (Atri *et al.*, 1993; Li and Rinzel, 1994; Keizer and DeYoung, 1994; Sneyd *et al.*, 1995; Tang *et al.*, 1996) and appears to agree well with experimental data. This gives

$$p\phi_1 x = \phi_{-1} y. \tag{9}$$

Thus, letting $h = x + y$, and recalling the conservation law (7) which now takes the form $h + z = 1$, we get

$$\frac{dh}{dt} = \phi_3(1 - h) - \left(\frac{\phi_1 \phi_2 p}{\phi_1 p + \phi_{-1}} \right) h. \tag{10}$$

The open probability of the receptor is now given by

$$P = \left(\frac{ph\phi_1}{\phi_1 p + \phi_{-1}} \right)^4. \tag{11}$$

We shall call this model the *two state receptor model*.

2.2   The whole-cell model

The two-state model of the IP_3 receptor can be incorporated into a model for intracellular Ca^{2+} dynamics by assuming that Ca^{2+} can enter the cell via two pathways; through the IP_3 receptor (with flux denoted by $J_{receptor}$), or through a generic leak from outside the cell or from the ER (J_{leak}), and is removed from the cytoplasm by Ca^{2+} ATPase pumps (J_{pump}). Thus, conservation of Ca^{2+} gives

$$\frac{dc}{dt} = J_{receptor} - J_{pump} + J_{leak}. \tag{12}$$

In choosing functional forms for J_{pump} and J_{leak} we follow previous models (reviewed in Sneyd *et al.*, 1995) and assume that J_{leak} is just a specified constant, while the Ca^{2+} ATPases work in a cooperative manner, with a Hill coefficient of 2, and thus

$$J_{pump} = \frac{V_p c^2}{K_p^2 + c^2}, \tag{13}$$

for some constants V_p and K_p. The flux through the receptor is given by the open probability multiplied by some scaling factor, and thus

$$J_{receptor} = k_f \left(\frac{ph\phi_1}{\phi_1 p + \phi_{-1}} \right)^4, \tag{14}$$
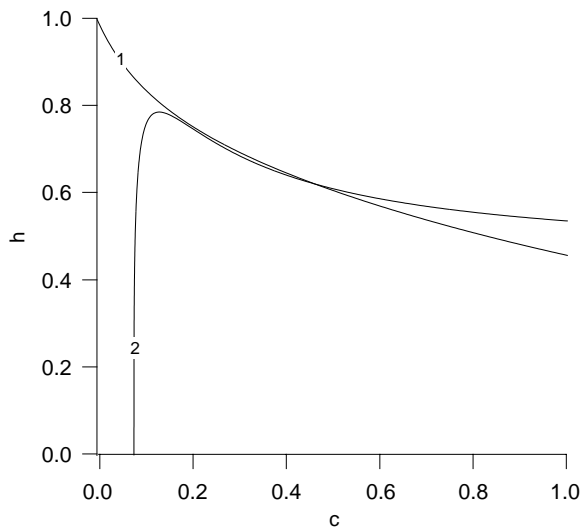
for some constant k_f.

Figure 2: Nullclines of the two–state model. Curve 1: $\frac{dh}{dt} = 0$. Curve 2: $\frac{dc}{dt} = 0$.

Note that this simplified whole-cell model now consists of only two differential equations, one for c, and one for h:

$$\frac{dh}{dt} = \phi_3(1 - h) - \left(\frac{\phi_1 \phi_2 p}{\phi_1 p + \phi_{-1}} \right) h, \tag{15}$$

$$\frac{dc}{dt} = k_f \left(\frac{p h \phi_1}{\phi_1 p + \phi_{-1}} \right)^4 - \frac{V_p c^2}{K_p^2 + c^2} + J_{\text{leak}}, \tag{16}$$

where the functions ϕ are given above.

2.3   Nullclines of the two-state model

The functions found in the two-state model are all derived from the kinetics of the IP$_3$ receptor, and take the rational forms dictated by the physiology. This complicated formulation makes analysis very difficult, and so a qualitative approximation of the model's behavior in a simpler form is desirable. Employing a method of simplification in the spirit of the FitzHugh-Nagumo reduction of the Hodgkin-Huxley equations, we look to the nullclines of the two-state model as the basis of the model's behavior. Much of the behavior of the two-state model can be traced back to the characteristic shape of its nullclines (Fig. 2). The nullcline $\frac{dh}{dt} = 0$ takes on an exponentially decaying shape, while the nullcline $\frac{dc}{dt} = 0$ rises sharply and then slowly decreases. Note that the nullclines are very nearly identical in the region $.1 < c < .5$. The similar behavior of the nullclines in this region makes their points of intersection extremely sensitive to changes in the value of p. As p increases, the nullclines intersect first at one point, then intersect at one point and are tangent in a second, then intersect at three points. After an interval of three intersections, the nullclines return to intersecting at only a single point. Since each of the intersection points of the nullclines gives a steady state, this behavior is clearly seen in a bifurcation diagram of the two-state model as an S-shaped curve of steady states.

Oscillations and waves in the two-state model have been discussed in detail by LeBeau *et al.* (1999) and by Sneyd *et al.* (2000), and we shall not repeat their arguments here. Suffice it to say that the model oscillations agree very well with experimental observations, and that a bifurcation analysis demonstrates the existence of a branch of stable isolated traveling waves, traveling at physiologically accurate speeds. This branch of traveling waves terminates at a T-point

(Glendinning and Sparrow, 1986), and an associated spiral of homoclinic bifurcations. It is our goal here to show that a simplified version of this model can be constructed, retaining the principal features of the model's behaviour.

3   Heuristic simplification of the two-state model

Although the two-state model exhibits interesting behavior when studied numerically, its functional forms are too complex for analytical study. It is therefore desirable to formulate a simpler model which exhibits the same behavior. Since the two-state model is already highly simplified from a physiological point of view, any further simplifications must be made using a heuristic approach. This simplification is in the spirit of the FitzHugh-Nagumo equations, which are based on the equations of Hodgkin and Huxley for describing the action potentials of the squid giant axon. The Hodgkin-Huxley equations are a landmark model in the history of excitable systems. They are based on a detailed understanding of the physiological behavior of the squid giant axon, and are soundly supported by experiment (Hodgkin and Huxley, 1952; Rinzel, 1990). They are also extremely complex and difficult to study, especially given the computational facilities available at the time of their conception. FitzHugh (1960, 1961, 1969) formulated a simplification of the Hodgkin–Huxley equations which qualitatively retains much of the same behavior as the original, complex model. Our approach to simplifying the two-state model will be similar, and relies upon a qualitative reproduction of the model's nullclines in functional forms unrelated to the original model equations.

3.1   Model equations

The primary information that the nullclines give us in any model is the position of the model's steady states for a given set of parameters. In the case of the two-state model, we have the goal of reproducing the S-shaped curve of steady states. To do so, the nullclines must intersect in one, two, or three points as the primary bifurcation parameter is varied. Furthermore, the global shapes of the nullclines should remain qualitatively unchanged.

The first step in simplifying the two-state model is to replace the nullcline $\frac{dh}{dt} = 0$ with a straight line, giving the equation

$$\frac{dh}{dt} = -c + (gh + p), \tag{17}$$

where p is the intercept of the nullcline, and acts as a primary bifurcation parameter. Replacing the nullcline of the two-state model with a straight line has an important ramification for the shape of the nullcline $\frac{dc}{dt} = 0$. In the original model, the two nullclines had a very similar curvature near their points of intersection. In order to keep the two nullclines nearly matching each other, a more sharply curved shape is necessary for the simplified nullcline than is found in the original model. This leads to the formulation

$$\frac{dc}{dt} = h - [e^{n_1 + n_2 c}(n_3 c^2 + n_4 c + n_5) + N_0], \tag{18}$$

where all parameters are constants given in Table 1. Note that, although we use the same variable, c and h, as in the full two-state model, they may no longer be given such a direct physiological interpretation. However, it is not too inaccurate still to think of c as a calcium concentration in some simplified model, and to treat h as an activation variable.

The nullclines now have the same qualitative behavior as the nullclines of the two-state model, which can be seen if we imagine the linear nullcline being swept across the nullcline $\frac{dc}{dt} = 0$ (Fig. 3). At low values of p, the nullclines intercept at a single point. As p is raised, they have one point of intersection and one tangent point, and then pass through a region with three points of intersection. As p continues to increase, the nullclines pass out of the region with three points of intersection, have a tangent point for a single value of p, and then return to one point of intersection.

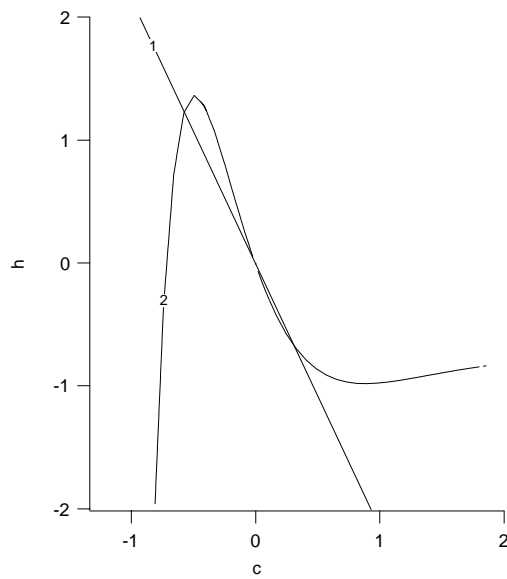| $n_1 = 1.732$	$n_2 = 3.466$
$n_3 = -0.882$	$n_4 = -0.252$
$n_5 = 0.132$	$N_0 = -0.7467$
$g = -0.335$	

Table 1: Parameters of the simplified model

Figure 3: Nullclines for the heuristic simplification of the two-state model. Curve 1: $\frac{dh}{dt} = 0$. Curve 2: $\frac{dc}{dt} = 0$.
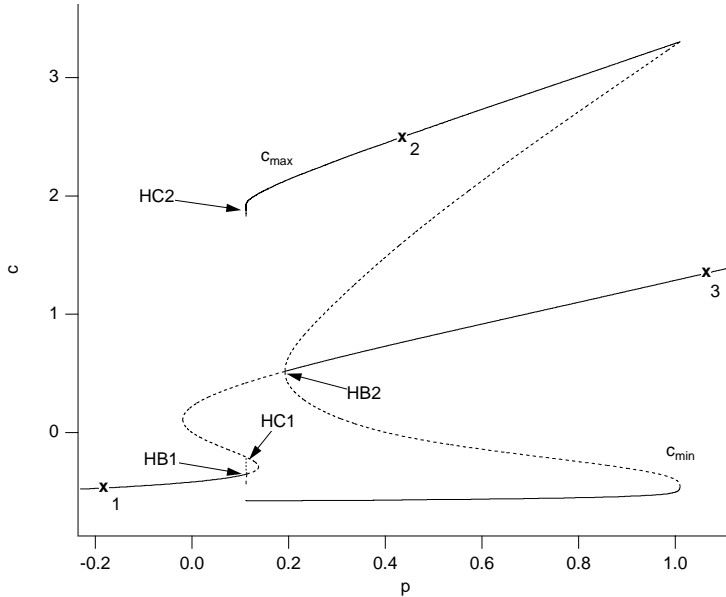
Figure 4: Bifurcation diagram of the simplified two-state model, showing the maximum and minimum of the periodic orbit as a function of a. HB — Hopf bifurcation; HC — homoclinic bifurcation. A broken line denotes instability.

3.2   Results

The simplified nullclines successfully reproduced the oscillations and steady state behavior of the original two-state model (Fig. 4). The curve of steady states has a clear S shape, with two limit points, as a result of the behavior of the nullclines as p is varied. For low values of p, the model has a single steady state. As p is increased, however, two branches of periodic orbits arise. The period of these orbits is very high near the homoclinic bifurcation, but decreases as the branches approach their termini in Hopf bifurcations. Bifurcations and orbits were tracked using the XPP/AUTO softwave package. We tracked period 1000 orbits as an approximation of homoclinic orbits. These results were found to be identical to those from orbits with period 2000, indicating that the orbits being tracked are very close to the homoclinic orbit.

3.3   Traveling waves

The primary focus of the two-state model is on producing traveling wave behavior which is physiologically realistic. In order to model this behavior in our simplified model, we simply substitute our model equations into the traveling wave ODEs for the two-state model. This gives us

$$c' = d, \tag{19}$$

$$d' = sd - h + e^{n_1 + n_2 c}(n_3 c^2 + n_4 c + n_5) + N_0, \tag{20}$$

$$sh' = -c + (gh + p) \tag{21}$$

where a prime denotes differentiation with respect to $\xi = x + st$. In this model, as in the two-state model, s acts as a secondary bifurcation parameter.

The bifurcations of principal interest are illustrated in Fig. 5, which shows the looped curve of Hopf bifurcations (labelled HB) in the s, p plane, as well as three branches of homoclinic orbits (labelled A, B, and C). The homoclinic branches B and C are very close together at higher values
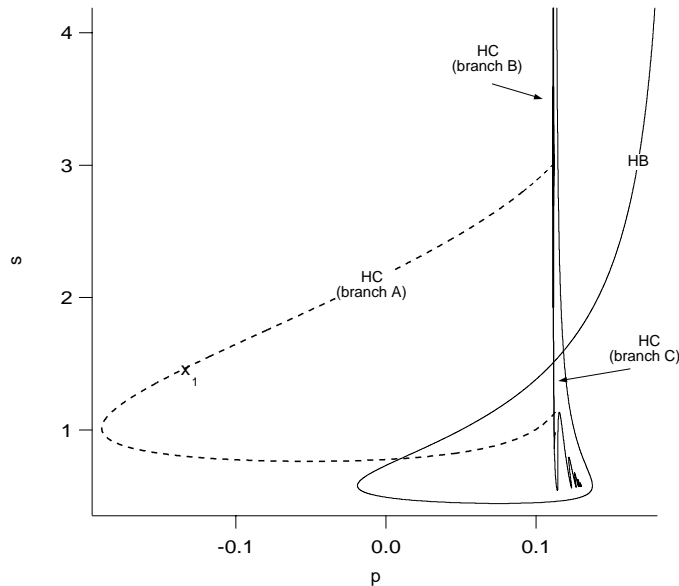
Figure 5: Two-parameter bifurcation diagram of the traveling wave equations for the heuristic simplification of the two-state model. HB denotes the curve of Hopf bifurcations, and HC denotes the branches of homoclinic bifurcations. Labeled point corresponds to homoclinic orbit in Fig. 8.

of s, so close as to be indistinguishable on the scale of the figure. However, although the distinction between branches B and C is not clear from the figure, we explain the important differences in more detail below.

3.3.1 The curve of Hopf bifurcations

If we continue the Hopf bifurcations at any fixed value of s through the s, p phase plane, a continuous, looped curve of Hopf bifurcations results (Fig. 5, curve HB). This loop, with two limit points, is a direct consequence of the S-shaped curve of steady states visible in the c, p phase plane at fixed values of s. As s varies, the Hopf bifurcations collide with the limit points of the steady state curves. Since the steady state curve constrains the possible positions of the Hopf bifurcations, this results in the limit points visible in Fig. 5.

3.3.2 Behavior as $s \to \infty$

The behavior of the simplified traveling wave model for very large s is exactly the behavior of the spatially homogeneous model (Fig. 4). Thus, a cross-section of the c, p phase plane at a constant, large, value of s shows two Hopf bifurcations (labeled HB1 and HB2 in Fig. 4) and two homoclinic bifurcations (HC1 and HC2 in Fig. 4). We note a number of things. Firstly, HB1 and HB2 both must necessarily lie on the curve labelled HB in Fig. 5; at higher values of s, HB1 lies on the left part of the curve HB, and HB2 lies on the right part. Secondly, HB1 is connected to HC1 by a branch of periodic orbits (as shown in Fig. 4), and HC1 lies on HC (branch C) of Fig. 5. Thirdly, HB2 is connected to HC2 by a branch of periodic orbits, and HC2 lies on HC (branch B) of Fig. 5. Thus branches B and C, although very close together, correspond to completely different homoclinic orbits, and are connected by branches of periodic orbits to different parts of the HB curve. Finally, we note that this diagram is not an exhaustive list of all the homoclinic bifurcations occuring in the model, as indeed there are infinitely many others not shown here. Nevertheless,
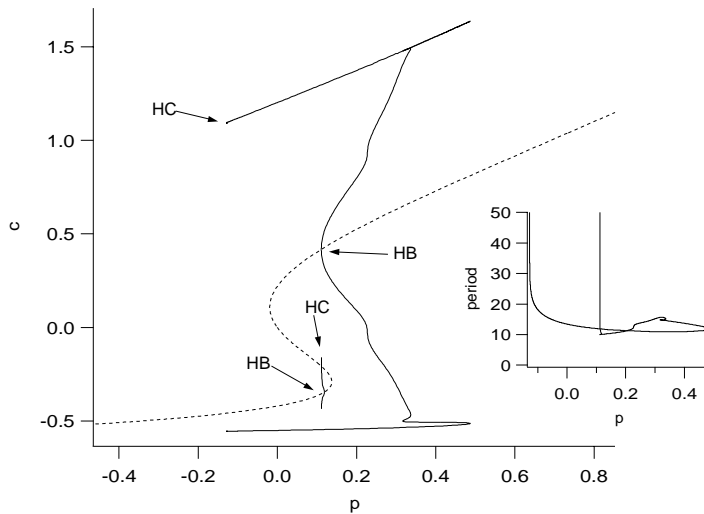
Figure 6: Bifurcation diagram for the traveling wave equations of the simplified two-state model, at a fixed value of $s = 1.5$. A broken line denotes the curve of steady states, while a solid line indicates the maximum and minimum values of c over a periodic orbit. Stability is not indicated. Inset shows the period of all orbits as a function of p.

the principal behaviour of the model can be well understood by consideration of only these three branches.

3.3.3   Homoclinic branch A

For intermediate values of s, the branch of periodic orbits arising from the right branch of HB (i.e., corresponding to HB2 in Fig. 4) no longer ends on branch B, but ends instead in a homoclinic bifurcation on branch A (Fig. 6). Thus, for intermediate values of s, the branch of periodic orbits extends to much lower values of p than is the case for higher values of s.

In the two-state model, branch A corresponds to physiologically occuring traveling waves, and so branch A of the simplified model is of great interest to us. Branch A has a positive slope in the s, p phase plane, indicating that wave speed increases with increased IP$_3$ concentration, which agrees with the two-state model and with experimental data from some cell types (Nathanson *et al.*, 1992). In other cell types such as hepatocytes and oocytes (Robb-Gaspers and Thomas, 1995; Lechleither and Clapham, 1992) the concentration of IP$_3$ does not appear to affect the intracellular calcium wave speed greatly. However, in more realistic models than the one presented here the predicted effect of IP$_3$ concentration on wave speed is small, and well within the observed experimental variability (Sneyd *et al.*, 1993, 2000). Outside the vicinity of the intersection with branch B, the homoclinic orbits of branch A show a simple baseline spike (Fig. 7, curve 1). This reflects the behavior of the orbit when viewed in the c, h phase plane. The homoclinic orbit begins at the saddle focus and makes a large amplitude orbit, returning to the saddle focus.

Branches A and B intersect in a T-point (Glendinning and Sparrow, 1986), a place where there exists a heteroclinic cycle. As the orbits approach the T-point along branch A their behavior changes (Fig. 7). As we enter the region in p where three steady states exist for a given s, two more steady states appear: an unstable node, and a saddle point. The orbits on branch A change in two significant ways as a result. First, the orbit in the c, h plane spends some time in the vicinity of the saddle point before returning to the saddle focus. Second, the orbit begins to spiral about the saddle focus before returning to it (curve 2). This is visible in the c, ξ plane as a transient
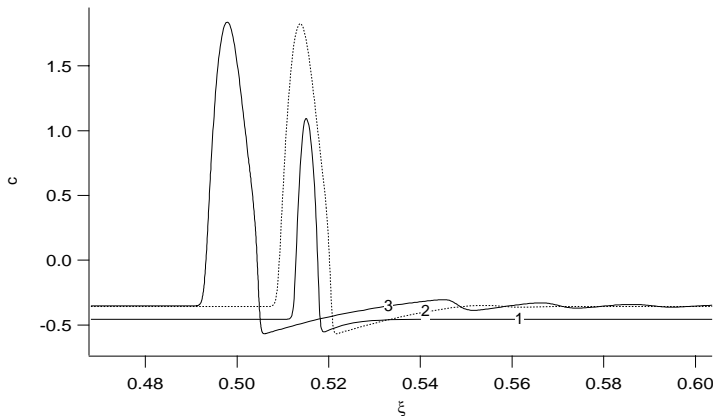
Figure 7: Homoclinic orbits approaching the T-point on homoclinic branch A.

elevation in the value of c after the main baseline spike, followed by a fall back to slight oscillations about the value of c corresponding to the saddle focus. The effect become more pronounced as orbits get closer to the T-point (curve 3).

3.3.4 Homoclinic branch B

Just as the homoclinic orbits of branch A approximate the heteroclinic connection of the T-point as they approach it, the orbits of branch B are affected by their proximity to the T-point. As predicted by Glendinning and Sparrow (1986), the linear branch A of homoclinic orbits is accompanied by a spiraling branch (branch B) of homoclinic orbits near the T-point; i.e., as branch B moves away from the T-point, it forms a spiral of homoclinic orbits. Since the spiral is compressed into a very small range of values of p, it can not be seen in Fig. 5. Furthermore, the homoclinic orbits on branch B approximate the heteroclinic connection differently than those on branch A. Whereas the homoclinic orbits of branch A "fall off" the saddle point and remain "attached" to the saddle focus, the orbits of branch B remain attached to the saddle point and fall off the saddle focus. If we approach the T-point along branch B, we see this clearly illustrated. At high values of s, the homoclinic orbit begins at the saddle point and makes a large amplitude orbit, returning to the saddle point (Fig. 8, curve 4). As s decreases, the time spent in the vicinity of the saddle focus increases (curve 5, curve 6). In the c, h plane (Fig. 8, B and C) the orbit begins at the saddle point, then proceeds to spiral about the saddle focus before making a large amplitude loop and returning to the saddle point. In the c, ξ phase plane, this appears as an oscillating tail preceding the main baseline spike, rather than following it as on branch A.

These behaviours are qualitatively identical to those seen in the full model, and thus we conclude that our simplified model does indeed retain the essential wave features found in the full model.

4 Discussion

Many models of cellular calcium dynamics have been conceived based on a physiological understanding of the mechanism of calcium release. In particular, LeBeau *et al.* (1999) have modeled the dynamics of the IP_3 receptor in pancreatic acinar cells. The numerical study of these models has been very successful, and has led to several testable predictions regarding calcium dynamics. The complex functional forms of these models, however, prohibit further analysis, even in the most simplified two-state model. It is thus desirable to find simplified models which exhibit the same behavior without retaining the functional forms necessary for a physiological model of the
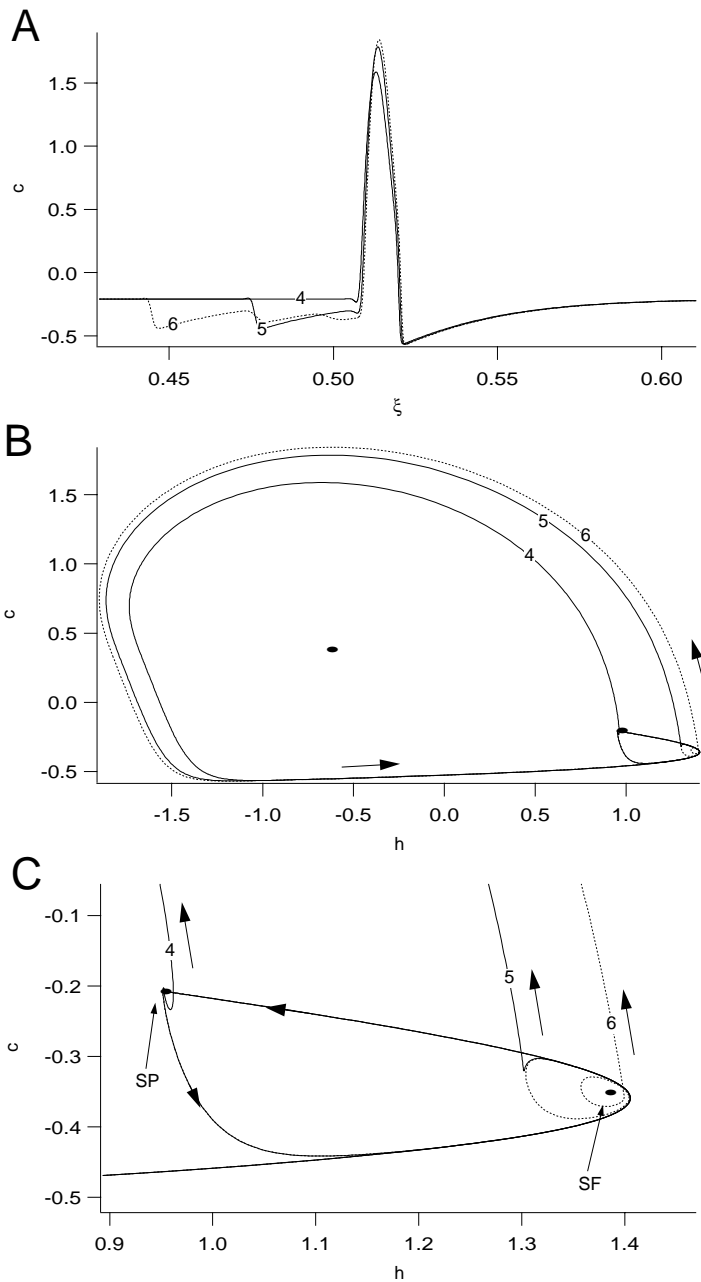
Figure 8: Homoclinic orbits approaching the T-point on homoclinic branch B. All orbits are at the fixed value of $s = 1.5$, but located on successive loops the spiral on branch B. A: Homoclinic orbits shown as a function of $\xi = x + st$. B: Homoclinic orbits shown in the c, h phase plane, illustrating the approach of the homoclinic orbit to an expected heteroclinic connection. C: An enlarged view of the c, h plane in the region of the saddle point and saddle focus. SP — saddle point. SF — saddle focus.

receptor. Following the approach of the FitzHugh-Nagumo simplification of the Hodgkin-Huxley equations, we constructed a heuristic simplification of the two-state model. We constructed qualitative approximations of the nullclines in the two-state model, and use these as the basis of both an oscillating model, and a traveling wave model.

Note that although we employed the approach of FitzHugh-Nagumo, the simplified model is not simply another variant of the widely studied FitzHugh-Nagumo system, but is an excitable system of a different type. Although we have not done a rigorous study, it appears that the behaviour of our simplified model is qualitatively similar to the behaviour of earlier models of calcium waves and oscillations, such as the model of Atri *et al.* (1993) or the model of Goldbeter *et al.*, (1990). For instance, the bifurcation diagram shown in Fig. 4 is qualitatively identical to the bifurcation diagram of the Atri model (Keener and Sneyd, 1998, Fig. 5.14), with a fold in the steady-state curve resulting in a homoclinic bifurcation close to the lower Hopf bifurcation. Furthermore, the bifurcation structure of the traveling wave equations of our model is very similar to that of the model of Goldbeter *et al.*, (1990), with traveling waves appearing as a curve of homoclinic bifurcations lying to the left of the curve of Hopf bifurcations. However, the bifurcation structure of traveling waves in the Goldbeter model has not been studied to the level of detail given here, and so it is not currently possible to determine exactly how similar the bifurcation structures are.

It is already well-known that the Goldbeter model is an excitable system of an unusual type (Sneyd *et al.*, 1993; Sneyd and Atri, 1993); for instance, traveling waves in that model do not obey the usual curvature-dependence of those in excitable systems of FitzHugh-Nagumo type. The model of Atri *et al.* also appears to behave differently from FitzHugh-Nagumo-type excitable systems, although there has been considerably less analysis done on that model. The simplified model presented here appears to incorporate, at least in a qualitative sense, the behaviour of both the Atri and the Goldbeter models, and thus we believe that a detailed analysis of this model will aid in a better understanding, not just of this model, but of the behaviour of a range of models of calcium wave propagation. However, this yet remains an open question.

It is interesting to note that there is not complete agreement about whether or not calcium dynamics in living cells really have properties that differ from the behaviour of generalised FitzHugh-Nagumo models. For instance, the models from Keizer's group (see, for instance, De Young and Keizer, 1992, and its simplifications) are usually of FitzHugh-Nagumo type, while the ones discussed above are not. The major difference is the assumptions made about the role of the concentration of calcium in the endoplasmic reticulum in terminating calcium release through the IP_3 receptor. In models where release is terminated entirely by receptor inactivation, the calcium dynamics seem to have some unusual properties, while other models, in which calcium release is terminated (at least in part) by a decrease in the endoplasmic reticulum calcium concentration, seem to behave similarly to the FitzHugh-Nagumo model. It is thus highly likely that both kinds of dynamic behaviour occur in cells, and that there is a continuum of behaviours between the two extremes.

Our approach was successful in reproducing all of the behaviors of the two-state model. The spatially homogeneous model exhibited the expected bifurcation behavior, with two homoclinic bifurcations and two Hopf bifurcations framing two branches of periodic orbits. In the traveling wave model, we successfully reproduced the looped curve of Hopf bifurcations and three branches of homoclinic bifurcations. Branch A, the stable branch of homoclinic orbits which, in the two-state model, corresponds to physiologically significant waves, has an increasing slope in the s, p phase plane. This means that an increased IP_3 concentration corresponds to an increased wave speed, an observed physiological characteristic of IP_3-mediated calcium waves. Two of these branches, A and B, intersect in a T-point. Near the heteroclinic connection of the T-point, the homoclinic orbits on branch A takes on an oscillating tail in addition to its primary wave. The amplitude of this oscillating tail may increase beyond the threshold of wave initiation, spawning new traveling waves. These secondary waves could then initiate tertiary waves, and so on. This behavior has been studied in detail in Sneyd *et al.* (2000) and is the underlying cause of an interesting kind of traveling wave instability, caused by the presence of the T-point.

References

[1] Atri, A., J. Amundson, D. Clapham and J. Sneyd. A single-pool model for intracellular calcium oscillations and waves in the *Xenopus laevis* oocyte. *Biophysical Journal.* 65: 1727–1739, 1993.

[2] Berridge, M. J. and A. Galione. Cytosolic calcium oscillators. *FASEB Journal.* 2: 3074–3082, 1988.

[3] Bezprozvanny, I. and B. E. Ehrlich. The inositol 1,4,5-trisphosphate ($InsP_3$) receptor. *Journal of Membrane Biology.* 145: 205–216, 1995.

[4] Cardy, T. J., D. Traynor and C. W. Taylor. Differential regulation of types-1 and -3 inositol trisphosphate receptors by cytosolic Ca2+. *Biochemical Journal.* 328: 785-93, 1997.

[5] Clapham, D.. Calcium signaling. *Cell.* 80: 259–268, 1995.

[6] De Young, G. W. and J. Keizer. A single pool IP_3-receptor based model for agonist stimulated Ca^{2+} oscillations. *Proc. Natl. Acad. Sci. USA.* 89: 9895–9899, 1992.

[7] Dupont, G. and A. Goldbeter. One-pool model for Ca^{2+} oscillations involving Ca^{2+} and inositol 1,4,5-trisphosphate as co-agonists for Ca^{2+} release. *Cell Calcium.* 14: 311–322, 1993.

[8] Dupont, G. and A. Goldbeter. Properties of intracellular Ca^{2+} waves generated by a model based on Ca^{2+}-induced Ca^{2+} release. *Biophysical Journal.* 67: 2191–2204, 1994.

[9] FitzHugh, R.. Thresholds and plateaus in the Hodgkin-Huxley nerve equations. *The Journal of General Physiology.* 43: 867–896, 1960.

[10] FitzHugh, R.. Impulses and physiological states in theoretical models of nerve membrane. *Biophysical Journal.* 1: 445–466, 1961.

[11] FitzHugh, R. (1969), *Mathematical models of excitation and propagation in nerve.* In: Biological Engineering, Ed: H. P. Schwan, McGraw-Hill, New York.

[12] Girard, S. and D. Clapham. Acceleration of intracellular calcium waves in *Xenopus* oocytes by calcium influx. *Science.* 260: 229-232, 1993.

[13] Glendinning, P. and C. Sparrow. T-points: A codimension two heteroclinic bifurcation. *Journal of Statistical Physics.* 43: 479–488, 1986.

[14] Goldbeter, A., G. Dupont and M. J. Berridge. Minimal model for signal-induced Ca^{2+} oscillations and for their frequency encoding through protein phosphorylation. *Proc. Natl. Acad. Sci. USA.* 87: 1461–1465, 1990.

[15] Goldbeter, A., *Biochemical oscillations and cellular rhythms: the molecular bases of periodic and chaotic behaviour*: Cambridge University Press, Cambridge, 1996

[16] Hajnóczky, G. and A. P. Thomas. Minimal requirements for calcium oscillations driven by the IP_3 receptor. *Embo Journal.* 16: 3533-43, 1997.

[17] Hodgkin, A. L. and A. F. Huxley. A quantitative description of membrane current and its application to conduction and excitation in nerve. *Journal of Physiology, London.* 117: 500–544, 1952.

[18] Keener, J. P. and J. Sneyd, *Mathematical Physiology*: Springer-Verlag, New York, 1998

[19] Keizer, J. and G. DeYoung. Simplification of a realistic model of IP_3-induced Ca^{2+} oscillations. *Journal of Theoretical Biology.* 166: 431–442, 1994.

[20] Kuba, K. and S. Takeshita. Simulation of intracellular Ca^{2+} oscillation in a sympathetic neurone. *Journal of Theoretical Biology.* 93: 1009–1031, 1981.

[21] Lechleiter, J. and D. Clapham. Molecular mechanisms of intracellular calcium excitability in X. laevis oocytes. *Cell.* 69: 283–294, 1992.

[22] Li, Y.-X. and J. Rinzel. Equations for $InsP_3$ receptor-mediated $[Ca^{2+}]$ oscillations derived from a detailed kinetic model: a Hodgkin-Huxley like formalism. *Journal of theoretical Biology.* 166: 461–473, 1994.

[23] Nathanson, M. H., P. J. Padfield, A. J. O'Sullivan, A. D. Burgstahler and J. D. Jamieson. Mechanism of Ca^{2+} wave propagation in pancreatic acinar cells. *Journal of Biological Chemistry.* 267: 18118-21, 1992.

[24] Parys, J. B., S. W. Sernett, S. DeLisle, P. M. Snyder, M. J. Welsh and K. P. Campbell. Isolation, characterization, and localization of the inositol 1,4,5-trisphosphate receptor protein in *Xenopus laevis* oocytes. *Journal of Biological Chemistry.* 267: 18776–18782, 1992.

[25] Petersen, C. C. H., E. C. Toescu and O. H. Petersen. Different patterns of receptor-activated cytoplasmic Ca^{2+} oscillations in single pancreatic acinar cells: dependence on receptor type, agonist concentration and intracellular Ca^{2+} buffering. *EMBO Journal.* 10: 527–533, 1991.

[26] Rinzel, J.. Electrical excitability of cells, theory and experiment: review of the Hodgkin-Huxley foundation and an update. *Bulletin of Mathematical Biology.* 52: 5–23, 1990.

[27] Robb-Gaspers, L. D. and A. P. Thomas. Coordination of Ca^{2+} signaling by intercellular propagation of Ca^{2+} waves in the intact liver. *The Journal of Biological Chemistry.* 270: 8102–8107, 1995.

[28] Rooney, T. A. and A. P. Thomas. Intracellular calcium waves generated by $Ins(1,4,5)P_3$-dependent mechanisms. *Cell Calcium.* 14: 674–690, 1993.

[29] Sneyd, J., S. Girard and D. Clapham. Calcium wave propagation by calcium-induced calcium release: an unusual excitable system. *Bulletin of Mathematical Biology.* 55: 315–344, 1993.

[30] Sneyd, J. and A. Atri. Curvature dependence of a model for calcium wave propagation. *Physica D.* 65: 365–372, 1993.

[31] Sneyd, J., J. Keizer and M. J. Sanderson. Mechanisms of calcium oscillations and waves: a quantitative analysis. *FASEB Journal.* 9: 1463–1472, 1995.

[32] Sneyd, J., A. LeBeau and D. Yule. Traveling waves of calcium in pancreatic acinar cells: model construction and bifurcation analysis. *Physica D*, in press

[33] Tang, Y., J. L. Stephenson and H. J. Othmer. Simplification and analysis of models of calcium dynamics based on IP_3-sensitive calcium channel kinetics.. *Biophysical Journal.* 70: 246–263, 1996.

[34] Thomas, A. P., G. S. J. Bird, G. Hajnóczky, L. D. Robb-Gaspers and J. W. J. Putney. Spatial and temporal aspects of cellular calcium signaling. *FASEB Journal.* 10: 1505–1517, 1996.

[35] Yule, D. I., E. Stuenkel and J. A. Williams. Intercellular calcium waves in rat pancreatic acini: mechanism of transmission. *American Journal of Physiology.* 271: C1285-94, 1996.